

Scanning Force Microscopy and Geometric Analysis of Two-Dimensional Collagen Network Formation

M. Mertig,^{1*} U. Thiele,¹ J. Bradt,¹ G. Leibiger,¹ W. Pompe¹ and H. Wendrock²

¹ Max-Planck-Arbeitsgruppe 'Mechanik heterogener Festkörper' an der Technischen Universität Dresden, Hallwachsstr. 3, D-01069 Dresden, Germany

² Institut für Festkörper- und Werkstofforschung Dresden, P.O. Box 16, D-01171 Dresden, Germany

Monomeric collagen films were prepared by spin-coating of acidic collagen solutions on different atomically flat surfaces. The thin biomolecular coatings have been investigated by scanning force microscopy. Depending on both the wetting behaviour and the microtopology of the substrates used, different film morphologies have been observed. Collagen monomers cover the surface of hydrophilic substrates homogeneously, whereas pore formation due to dewetting processes takes place at non-structured hydrophobic surfaces. The size of pores depends on the evaporation velocity of the solvent during spin-coating. Topological and metric properties of the resulting networks have been analysed and compared to soap foam network structures. © 1997 by John Wiley & Sons, Ltd.

Surf. Interface Anal. 25, 514–521 (1997)

No. of Figures: 9 No. of Tables: 0 No. of Refs: 26

KEYWORDS: monomeric collagen; film formation; network structures; dewetting; scanning force microscopy

INTRODUCTION

Currently, in medicine, much effort is made for the development of biocompatible implant materials. However, the design of the interface between the living organism and synthetic implant material is still an unsolved problem because, in most cases, implant materials do not provide durable adherent contact; the implant will be embedded only in a non-adherent fibrous capsule. Therefore, novel concepts focus on the design of bioactive interfaces, which may induce bonding between the synthetic material and the surrounding tissue.¹ Here, the study of interaction between the first biomolecular monolayer and solid-state surfaces with different chemical, physical and morphological properties is of great interest. Therefore, we have studied the formation of thin biomolecular coatings. In this paper we present the first results of the investigation of structure formation in monomeric collagen I films at different atomically flat surfaces.

Collagen I is the major organic constituent of bone. The collagen I molecule could mediate the binding of osteoblasts to a substrate because it contains cell adhesion sites.² Osteoblasts are cells that are responsible for bone synthesis. A collagen I monomer consists of three peptide chains wound into a triple helix. The molecule is rod-shaped with a length of 300 nm and a diameter of 1.5 nm as measured by x-ray diffraction.³ The molecular weight is ~300 kDa. At physiological conditions collagen monomers assemble to fibrils, which are relatively

stiff filamentous aggregates. They can become several hundred micrometres long. Monomeric protein can be obtained by dissolving collagen fibrils from young tissue in acetic acid. We have deposited monomeric collagen films on different solid-state surfaces by spin-coating of acidic collagen I solutions.

The films have been investigated by scanning force microscopy (SFM), which allows molecular resolution imaging of biological macromolecules (for a review, see Ref. 4). Until now, only a few attempts have been made to resolve collagen monomers adsorbed onto mica by SFM.^{5,6} Structure formation of monomeric collagen films has not been investigated yet.

We have observed a network pattern in collagenous films on non-structured hydrophobic substrates. Pore formation due to dewetting of the spread volatile solvent is assumed to cause patterning. The investigation on collagen films allows information to be obtained about dewetting phenomena of a volatile liquid solution under the influence of rod-like macromolecules.

For a more quantitative characterization of the geometrical film properties, the imaged cellular pattern has been analysed by mathematical methods^{7,8} developed to describe random tessellations by their topological and metrical properties, such as cell area and cell perimeter, edge length, angle between the edges, edge number and vertex coordination number. The results achieved will be compared to networks of aged soap foam.

EXPERIMENTAL

Monomeric collagen solutions with protein concentrations of 0.002–0.2 mg ml⁻¹ have been prepared by dissolving collagen I from calf skin (Fluka, Buchs,

* Correspondence to: M. Mertig, Max-Planck-Arbeitsgruppe 'Mechanik heterogener Festkörper' an der Technischen Universität Dresden, Hallwachsstr. 3, D-01069 Dresden, Germany.

Contract grant sponsor: Bundesministerium für Bildung, Wissenschaft, Forschung und Technologie; grant no. 0310812.

Switzerland) in 0.1 M acetic acid (pH \sim 3) under stirring for several hours at 4 °C.

The thin collagen films were prepared by spin-coating at room temperature: an \sim 30 μ l drop of collagen solution was placed onto the substrate for 60 s. Then, spinning of the substrate was started at \sim 5000 rpm. Working at room temperature in ambient air, the films dried usually within \sim 10 s. In most cases the spin duration was 60 s. In some experiments, the evaporation velocity of the solvent was reduced: either 0.1 M acetic acid was dropped continuously onto the spinning sample during half of the spinning duration or spinning was carried out for 60 s at relative humidity near 100%.

Mica, highly oriented pyrolytic graphite (HOPG) and Au(111) surfaces have been employed as substrates, with a size of \sim 1 cm². Mica and HOPG were freshly cleaved immediately before spin-coating. The Au(111) substrates were prepared by epitaxial growth of an Au layer on freshly cleaved mica. The preparation method is described in more detail elsewhere.⁹ The collagen film on the gold sample was settled immediately after the substrate was exposed to air. The wetting properties of the substrates were quantified by measuring the contact angles of a standing drop of collagen solution on the substrate. Contact angles of 0°, 75° and 60° have been determined for mica, HOPG and Au(111), respectively. The dry collagen films were examined by SFM. Images were obtained using a commercial multimode microscope (NanoScope IIIa, Digital Instruments, Santa Barbara) operated at \sim 300 kHz in tapping mode under ambient environmental conditions (<40% relative humidity). Tapping mode provides 'gentle' imaging of the biomolecular film, because lateral forces to the specimen are circumvented. Scanning at a scan rate of \sim 1 Hz (lines s⁻¹) was performed with silicon tip cantilevers (NanoProbe™, 125 μ m) at a minimum 'tapping' force. All images (512 \times 512 pixels) shown in this paper are presented essentially unfiltered; in some cases, the 'Flatten' filter of the NanoScope software was used. Images display height mode or amplitude mode in topview. The latter is recorded simultaneously with the height signal. The amplitude signal is analogous to the deflection signal in the conventional error signal mode.¹⁰ It allows small corrugations of the sample to

be resolved and has therefore been applied successfully to protein imaging.¹¹

To quantify the geometrical properties of the observed network structures, the image analyser QUANTIMET 570 (Leica, Bensheim, Germany) was employed in combination with a self-written analysis program. The SFM image is transformed to a computer internal representation used to determine single-cell properties such as cell area, cell perimeter, edge length and angles between the edges, as well as correlation properties like the number of neighbouring cells of every individual cell, etc. All distribution and correlation functions were calculated from the transformed 512 \times 512 \times 8 bit SFM images, considering only bulk cells, which means, that open cells at the edges of the SFM images have been neglected in the analysis.

RESULTS

The collagen coatings obtained are very thin (<15 nm) and fine structured. For this reason, SFM appears to be a unique method for investigating monomeric films.

Figure 1 shows the topography of a collagen film prepared on mica with a starting collagen concentration of 0.2 mg ml⁻¹. Collagen covers the surface homogeneously. The monomers form a felt-like structure of randomly deposited molecules. The topography of the sample is very smooth, indicating a constant collagen film thickness. The height of the observed surface corrugations is 0.5–1.0 nm, corresponding to about half of the molecule diameter. Lowering the content of collagen in the solution, the felt-like structure changes into a random distribution of individual monomers at the surface. Figure 2 shows an image of a sample prepared from a solution with 0.002 mg ml⁻¹ collagen. We observed that, typically, only a small part of the collagen monomers appears fragmented, which is a sign of the high purity of the collagen used and indicates that the monomers do not undergo denaturation during film preparation. The imaged molecules have a length of 300 nm. The height of the molecules was measured to be 0.6–0.9 nm, which is less than the diameter reported

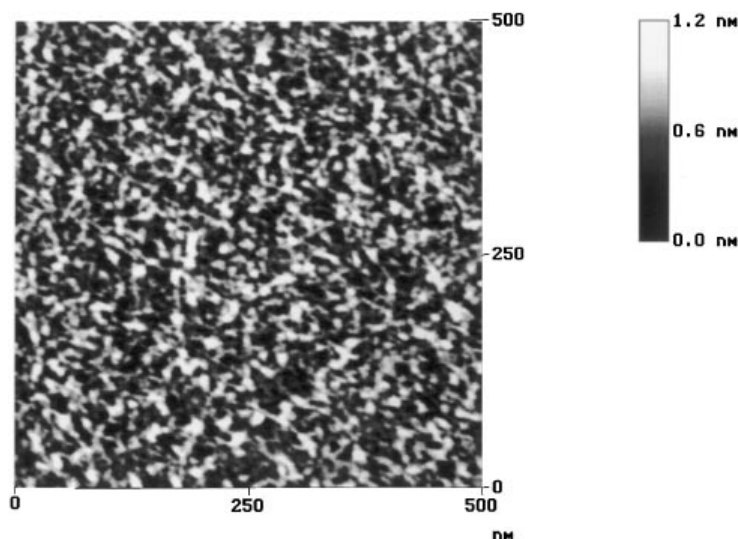


Figure 1. The SFM image of a collagen film on mica. Collagen concentration of the liquid precursor is 0.2 mg ml⁻¹.

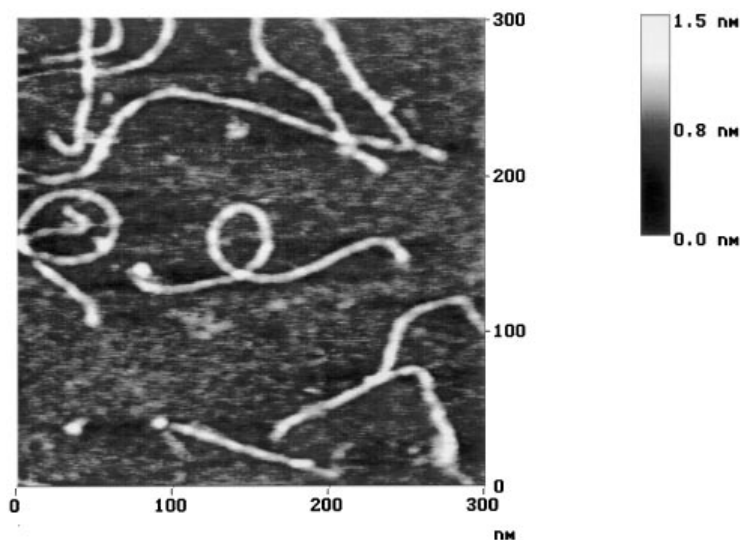


Figure 2. Image of collagen monomers adsorbed onto mica. Collagen concentration of the liquid precursor is 0.002 mg ml^{-1} .

from x-ray diffraction measurements.³ We assume that flattening of molecules takes place by surface tension during drying. Coulomb forces between positively charged monomers at pH 3 (isoelectric point of collagen ~ 9)¹² and negatively charged mica seem unlikely to explain the observed flattening effect. The width of the collagen monomers will appear broadened by the radius of the SFM tip. We have determined a width of the monomers of $< 11 \text{ nm}$ (at substrate level), indicating a tip radius of $< 10 \text{ nm}$.

Figure 3 shows a collagen coating prepared on HOPG with a starting concentration of 0.2 mg ml^{-1} . Comparison to (Fig. 1) clearly shows that film formation differs completely at hydrophobic and hydrophilic substrates. On hydrophobic, non-wetting surfaces a network structure with 'open' patches/pores is formed. At pore sites no collagen is deposited at the surface. The average diameter of the patches is $\sim 380 \text{ nm}$ and they are surrounded by collagen rims of height $6\text{--}8 \text{ nm}$, which is a factor of 3–4 larger than the collagen film

height in-between the patches. Figure 4 shows more detail of the same sample taken at higher resolution in the amplitude mode. In this mode a fine structure oriented along the rims is visible. This suggests that collagen monomers are arranged parallel in the observed rims.

Unfortunately, SFM does not allow film formation to be studied *in situ*; the coatings are always examined in their final state. Nevertheless, because the images obtained represent 'snapshots' of the developing structure at that moment, when the solvent is completely evaporated, it is possible to follow the process of film formation by controlling the evaporation speed of the solvent. By keeping the sample wet or in higher humidity during spin-coating, more highly developed structures can be fabricated. This fact is illustrated in (Fig. 5), which shows an image of a sample prepared under the same conditions as that of (Fig. 3), except that 0.1 M acetic acid was dropped continuously onto the spinning sample during the first 30 s of spin-coating. This sample

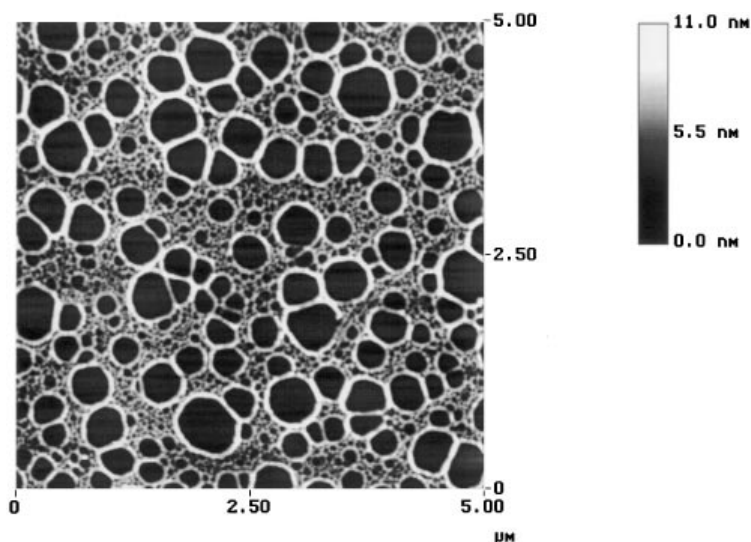


Figure 3. Image of a collagen film on HOPG. The film exhibits patches where no collagen is adsorbed. The characteristic diameter of the patches is $\sim 380 \text{ nm}$. Collagen concentration of the liquid precursor is 0.2 mg ml^{-1} .

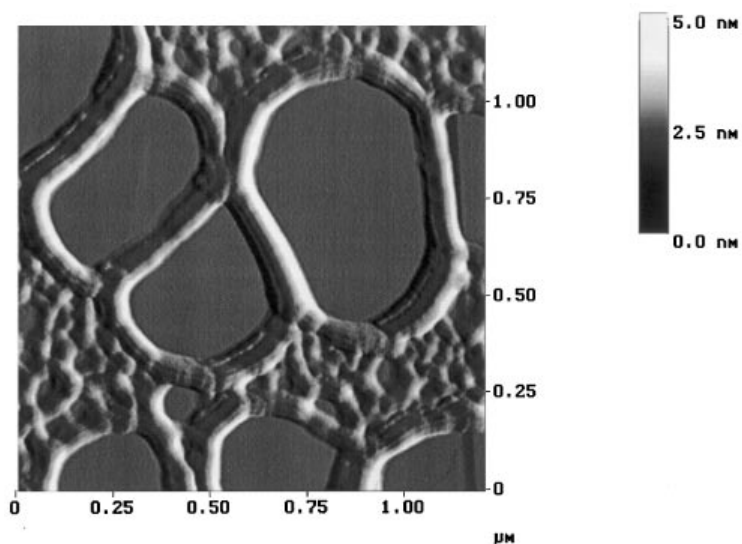


Figure 4. The SFM image (amplitude mode) of a collagen film on HOPG. Same preparation as for the sample shown in (Fig. 3). Small corrugations directed along the rims of the patches are visible, indicating a parallel orientation of monomers in the rims.

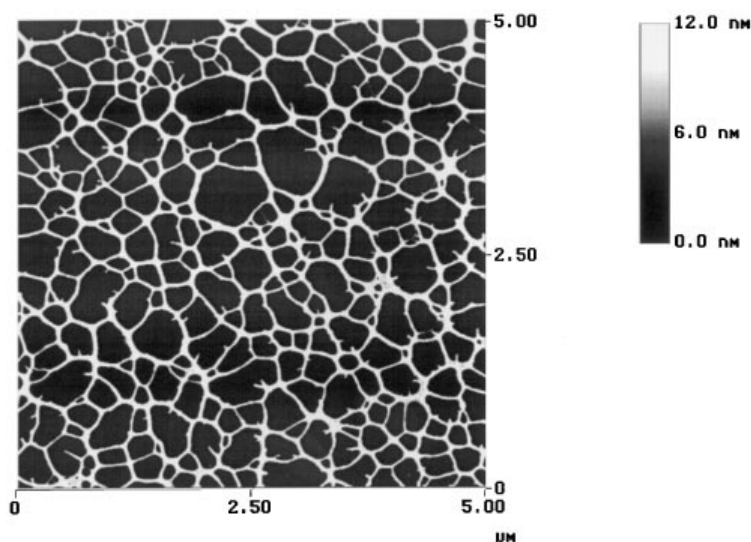


Figure 5. Image of a 'developed' collagen film on HOPG. For preparation, see text. The sample exhibits a polygonal network of thin collagen lines/edges.

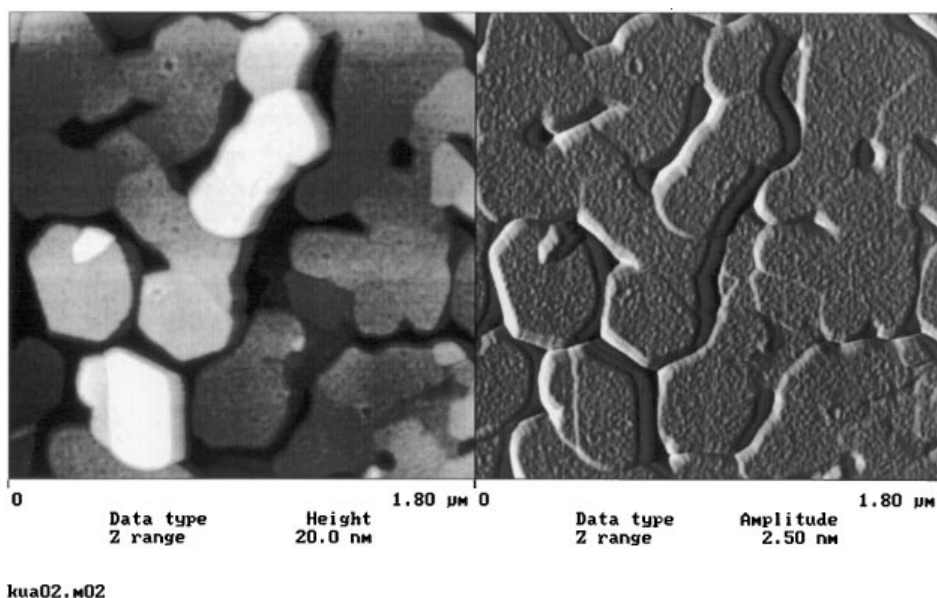


Figure 6. The SFM image (left: height mode; right: amplitude mode) of a collagen film on an Au(111) surface with a terrace-like structure. The collagen film appears interrupted at the edges of the terraces. Collagen concentration of the liquid precursor is 0.2 mg ml⁻¹.

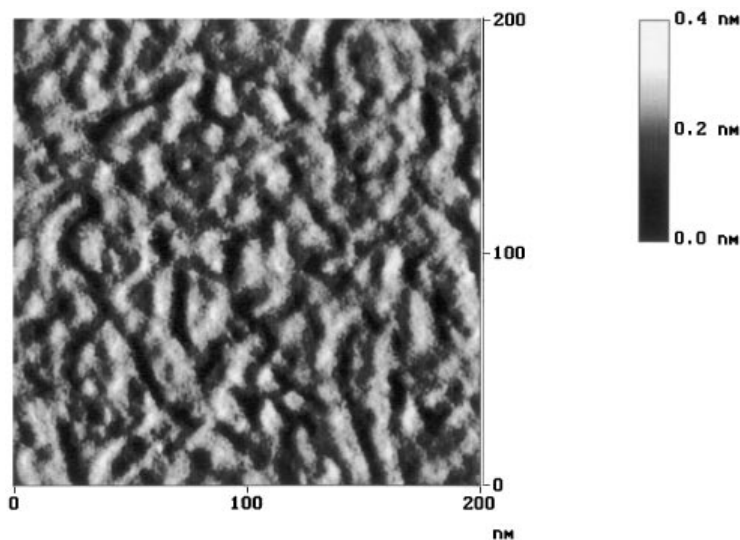


Figure 7. Same sample as in (Fig. 6) but at a higher resolution (amplitude mode).

exhibits a more developed network structure that resembles the polygonal network pattern of two-dimensional soap foam.^{13–16} Comparison to (Fig. 3) suggests that the pores in the film have grown until the rims of neighbouring pores came into contact and form one common rim. It should be mentioned that the distribution of pore sizes is relatively narrow, indicating a more or less simultaneous emergence of pores in the collagen film that is forming.

In (Fig. 6) an image of the Au(111) surface covered with a collagen film prepared from a starting concentration of 0.2 mg ml^{-1} is shown, in height mode (left) and amplitude mode (right). The Au(111) sample consists of atomically flat ‘terraces’ with an average diameter of $\sim 400 \text{ nm}$, determined from the power spectral density

of the image. The terraces exhibit different heights. The full width at half-maximum of the height signal distribution is $\sim 10 \text{ nm}$. The amplitude image shows clearly that the collagen film covers all terraces homogeneously, but separately. Only the edges of the terraces are uncovered. This allows the thickness of the coating to be determined (3.5 nm). Figure 7 shows the collagen film at a terrace at higher resolution in amplitude mode. Here, again, we observe a felt-like structure similar to that on mica.

Samples that exhibit a well-developed polygonal network structure, as shown in (Fig. 5), can be regarded as examples of cellular pattern or random tessellations. They can be analysed quantitatively by means of mathematical methods of stochastic geometry.^{7,8} Evolution of two-dimensional soap foam was studied extensively^{13–16} by applying similar methods. Therefore, a variety of data exist with which to compare collagen networks.

Before data analysis the SFM images obtained have been processed to produce an exact computer internal representation of the network. The latter contains all coordinates of network vertices and information about existing lines between them. In this representation the real width of rims has been neglected. In (Fig. 8) the computer internal representation of the polygonal network of the bulk cells matching the SFM image of (Fig. 5) is given. It can be seen that the resemblance achieved is very close. From this representation the statistical distributions of metric and topological properties characterizing single cells, as well as correlations between them, are calculated. In order to acquire sufficient statistics, several SFM images of the same sample were analysed. The total number of analysed cells for one set of data was always more than 700.

Examples for the metric and topological network analysis are shown in (Fig. 9). Figure 9(a) gives the distribution functions of the perimeters of single cells for two developed collagen networks prepared in different ways. The first sample (hollow circles) is the same as already shown in (Fig. 5). Here, the SFM image represents only one-third of the analysed part of the

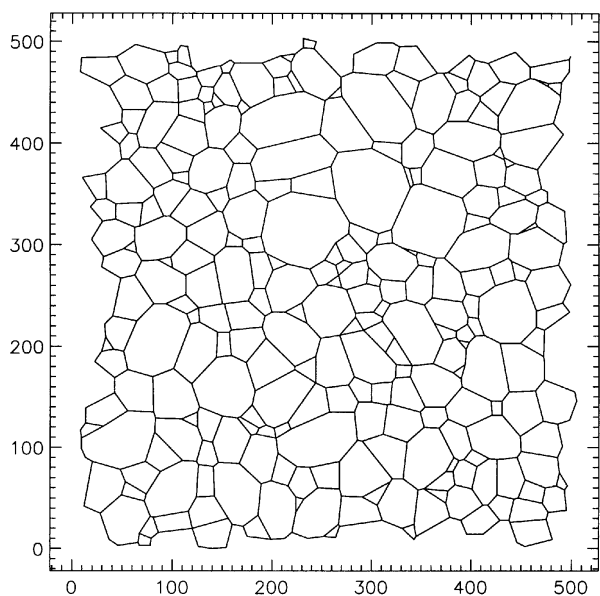


Figure 8. Computer internal representation of the SFM image shown in (Fig. 5). The axes are given in pixel units. The pixel size is 9.77 nm .

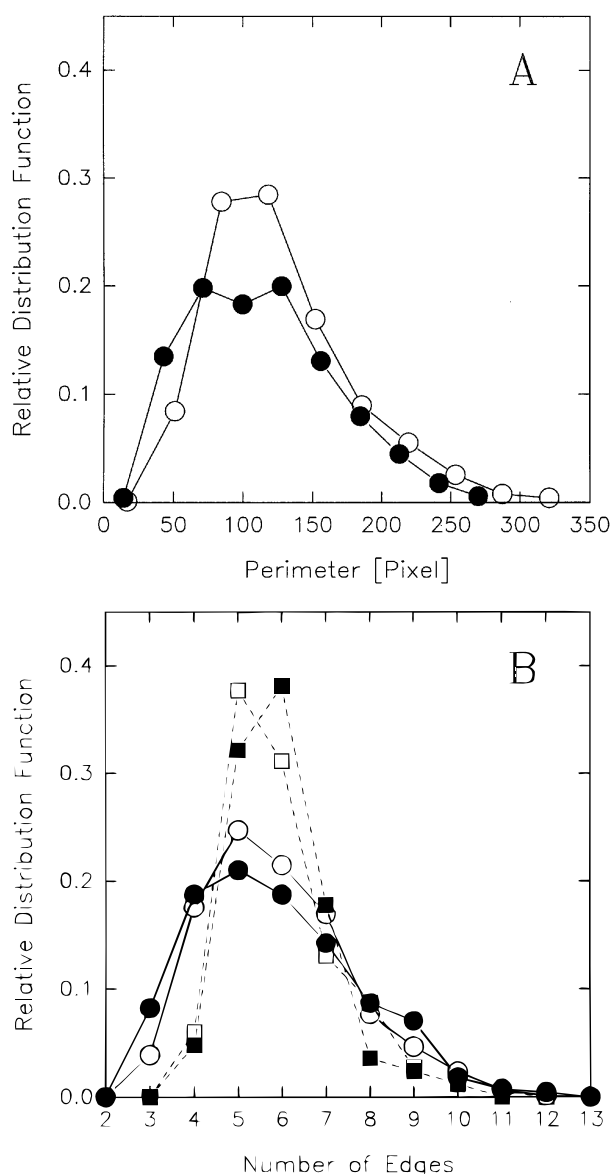


Figure 9. Relative distribution functions of developed two-dimensional collagen networks and soap foam: (a) distribution of perimeters (pixel size is 9.77 nm); (b) distribution of edge numbers. Circles indicate collagen; for preparation, see text. Squares indicate soap foam; hollow squares, Ref. 13; filled squares, Ref. 14.

sample. The second sample (filled circles) was prepared by spin-coating for 60 s under a humidity of near 100%. Both perimeter distribution functions are very similar in shape and length scale. The average perimeters of samples 1 and 2 are 1.17 and 1.28 μm , corresponding to average diameters of 372 and 407 nm, respectively. The second moments of the distribution functions are 0.27 and 0.25 μm^2 , respectively.

Figure 9(b) compares the distribution of the edge numbers of the cells of the two collagen samples with those of aged two-dimensional soap foam taken from two different sources.^{13,14} It is clearly seen that the distribution functions of collagen networks as well as the distribution functions of the two soap foams are respectively similar among one another. The second moments of the soap foam distributions are ~ 1.4 , whereas we

calculated 3.7 and 2.8 for the two collagen samples, respectively, i.e. the distribution functions for soap foam are very narrow in comparison to those determined for collagen.

DISCUSSION

It was the intention of the work presented in this paper to study the dependence of structure formation in thin spin-coated collagen films on various parameters, including properties of the substrate and the liquid precursor. In these investigations we observed that the structure of the biological coatings can be influenced in a controlled manner. First of all, we found a clear difference in the film structures obtained when working with hydrophilic and hydrophobic substrates. Hydrophilic substrates yield smooth, homogeneous coatings of randomly distributed collagen monomers. The biomolecular film exhibits a felt-like structure. On non-structured hydrophobic substrates pronounced pattern structures are formed. On Au(111) surfaces we perceived that film patterning on a hydrophobic surface can be suppressed by the occurrence of a notable microtopology of the substrate. Secondly, we could show that decreasing the evaporation velocity of the solvent by keeping the sample wet or at higher humidity during spin-coating leads to more highly developed structures. Sample preparation under fixed experimental conditions yields fairly reproducible structures.

The second purpose of this work was to elucidate the process of pattern formation in collagen films on hydrophobic substrates. These structures are the result of a complex process involving spreading of the drop, drying of the collagen solution, rupture and dewetting of the film. Different morphologies that depend on the collagen concentration of the liquid precursor have been observed. In this paper, we concentrate on an outline of the ongoing processes. A detailed, more quantitative analysis will be presented elsewhere.¹⁷

In the first stage of spin-coating the precursor is spread over the sample to form a liquid film with homogeneous thickness. Knowing the collagen concentration in the precursor and evaluating the amount of collagen deposited at the surface in the final state as measured by SFM, we can estimate the starting precursor film thickness after spin-off to $\sim 10 \mu\text{m}$.

In the second stage the liquid precursor film gets thinner by evaporation of the solvent. This process is accompanied by an enormous increase of both collagen concentration and viscosity of the precursor.

The third step is rupture of the film. As described in the literature, two different mechanisms^{18–22} seem to be possible here: the nucleation of individual pores or the almost simultaneous occurrence of multiple pores driven by surface undulations (bifurcation-type instability). Following the concept of Brochard-Wyart *et al.*,^{19,21} both regimes should occur at different film thicknesses. They define a critical thickness $h_R \sim 100 \text{ nm}$; above this value pore nucleation is the dominant process. At thicknesses much below h_R spontaneous growth of surface undulations should take place and cause a simultaneous multiple film rupture. It should,

however, be mentioned that the collagen film formation does not happen as an equilibrium process at constant thickness. Fast evaporation drives the system to smaller film thickness during rupture. Therefore, it is questionable whether the concept of a critical film thickness is directly applicable to our experiment. At the moment we cannot distinguish between avalanche-like nucleation or bifurcation-type instability. Nevertheless, we did not perceive the occurrence of individual pores much larger than average, which means that, independently of the origin of rupture, it takes place nearly simultaneously at multiple sites. In the context of fast evaporation, this would mean that rupture takes place in a defined region of film thickness.

The upper limit of film thickness leading to rupture can be estimated easily. In the simplest possible assumption, nucleated pores in the film will grow if their radius is larger than a critical radius $r_c = h/\sin\Theta$, where h is the film thickness and Θ is the wetting angle. Thus, rupture occurs at a film thickness smaller than r_c . The critical pore radius has to be smaller than the observed average pore radius of network cells, which is ~ 190 nm in our case. Therefore, we can estimate the upper film thickness for rupture to be < 190 nm. However, taking into account the necessary pore growth to develop a polygonal network, we suppose that rupture takes place at a thickness much below the estimated upper limit. This presumption is supported by the following observation. The investigations with Au(111) surfaces have shown that film rupture does not arise in the case of a terrace-like microtopology of the surface. We suppose that the presence of terraces with a characteristic lateral dimension comparable to the average diameter of the usually observed pores and with different height levels causes an unloading dissection of the precursor film before rupture occurs. In this case the thin-spread film 'relaxes' from the edges of the terraces and, consequently, pore formation is suppressed. In general, this would indicate that the rupture of collagen films takes place at a film thickness in the region of < 10 nm.

The fourth stage of film formation is pore growth. In this process transport of collagen monomers is caused by dewetting. They are pushed away, forming a wall around the pore. The size of the developing pore depends on the time remaining after pore formation until that moment when the solvent is completely evaporated. At collagen concentrations of 0.2 mg ml^{-1} we have observed that circular pores are formed at the beginning of pore growth. The SFM measurements have shown that the monomers are arranged parallel in the pore walls. With increasing duration of evaporation of the remaining solvent after film rupture, the patterned film develops towards a polygonal network.

The third purpose of this paper was to analyse quantitatively the polygonal pattern formed by collagen molecules and to draw conclusions from these data for understanding the process. The close similarity in shape and length scale of the two collagen curves in both plots of (Fig. 9) implies that the resulting structures are only little effected by the different preparation procedures. The relatively narrow distribution of the cell perimeters [Fig. 9(a)] and, consequently, the distribution of pore sizes indicate a nucleation of all pores at nearly the same time. In other words, the time dependence of the

pore nucleation rate should have a clear maximum. A constant or, in time, growing nucleation rate would lead to much broader distributions of the metric cell properties.

On the other hand, collagen networks are more disordered than other investigated networks, such as two-dimensional soap foams and polygonal networks of thin polymer films occurring as an intermediate state in dewetting.²³⁻²⁵ As usual, the second moment of the edge number distribution is taken as a measure of disorder.¹³ The distribution functions for collagen are broader than for soap foam [Fig. 9(b)]: first, the probability of occurrence of cells with three and four edges is much higher for collagen than for soap foam; secondly, the probability for cells with large numbers of edges decreases more slowly for collagen networks. This is connected with the geometry of the 300 nm long collagen molecule. The liquid collagen precursor has to be considered as a 'structured' liquid, whereby the length of the dissolved molecules is comparable to the characteristic scale of network cells. In soap foam and polymer films the building elements of the network are much smaller than the network structures. Using structured precursors like collagen solutions, very stable networks are generated. On the contrary, the networks prepared by dewetting of thin polymer films decay finally via a Rayleigh instability into rows of drops.^{24,26} The higher disorder in collagen films results from suppression of local equilibration processes by the presence of collagen molecules. There will be no absorption of short edges into the neighbouring edges, no disintegration of fourfold vertices into two threefold vertices and no coagulation of smaller cells through rupture of thin edges between them.

CONCLUSIONS

Investigating spin-coated collagen films on atomically flat surfaces by SFM, we found that structure formation at room temperature mainly depends on the wetting behaviour and the microtopology of the substrate, the collagen concentration of the precursor and the evaporation velocity of the solvent. By controlling these factors, coatings with different topological and metric properties can be prepared fairly reproducibly. Non-structured hydrophobic substrates are especially suited for the fabrication of patterned coatings. Pattern formation is proposed to be driven by dewetting of the film after nucleation of pores in the drying precursor film. The geometric analysis of the resulting network structures yields information about the film formation processes and the influence of the collagen molecules. Results of the analysis imply a nearly simultaneous occurrence of all pores and oppression of pore coalescence.

Acknowledgements

We wish to thank T. Fritz for preparation of the Au(111) substrates and B. Winzer for valuable assistance in an early stage of the experiment. We are grateful to G. Keßler and M. Fischer for helpful and encouraging discussions.

This research was partly supported by the Bundesministerium für Bildung, Wissenschaft, Forschung und Technologie (BEO), contract no. 0310812.

REFERENCES

1. L. L. Hench and J. Wilson, in *Advanced Series in Ceramics*, edited by M. McLare and D. E. Niesz, Vol. 1, p. 1. World Scientific, Singapore (1993).
2. G. B. Fields, *Connect. Tiss. Res.* **31**, 215 (1995).
3. A. J. Hodge, in *Treatise on Collagen*, edited by G. N. Ramachandran, Vol. 1, pp. 185 and 205. Academic Press, New York (1967).
4. H. G. Hansma and J. H. Hoh, *Annu. Rev. Biophys. Biomol. Struct.* **23**, 115 (1994).
5. E. A. G. Chernoff and D. A. Chernoff, *J. Vac. Sci. Technol. A* **10**, 596 (1992).
6. M. Gale, M. S. Pollanen, P. Markiewicz and M. C. Goh, *Biophys. J.* **68**, 2124 (1995).
7. R. V. Ambartzumjan, J. Mecke and D. Stoyan, *Geometrische Wahrscheinlichkeiten und Stochastische Geometrie* (in German). Akademie Verlag, Berlin (1993).
8. H. Hermann, *Stochastic Models of Heterogeneous Materials*. Trans. Tech. Publications Ltd., Zürich (1991).
9. T. Fritz, M. Hara, W. Knöll and H. Sasabe, *Mol. Cryst. Liq. Cryst.* **253**, 269 (1994).
10. C. A. J. Putman, K. O. van der Werf, B. G. de Groot, N. F. van Hulst, J. Greve and P. K. Hansma, *Proc. SPIE* **1939**, 198 (1992).
11. M. Fritz, M. Radmacher, M. W. Allersma, J. P. Cleveland, R. J. Stewart, P. K. Hansma and C. F. Schmidt, *Proc. SPIE* **2384**, 150 (1995).
12. M. Iijima, Y. Moriwai and Y. Kuboki, *J. Cryst. Growth* **137**, 553 (1994).
13. D. Weaire and N. Rivier, *Contemp. Phys.* **25**, 59 (1984).
14. J. A. Glazier, M. P. Anderson and G. S. Grest, *Philos. Mag. B* **62**, 615 (1990).
15. J. A. Glazier, S. P. Gross and J. Stavans, *Phys. Rev. A* **36**, 306 (1987).
16. W. Y. Tam and K. Y. Seto, *Phys. Rev. E* **53**, 877 (1996).
17. J. Bradt, M. Mertig, W. Pompe, U. Thiele and B. Winzer, in preparation.
18. E. Ruckenstein and R. K. Jain, *J. Chem. Soc. Faraday Trans. II* **70**, 132 (1974).
19. F. Brochard-Wyart and J. Daillant, *Can. J. Phys.* **68**, 1084 (1989).
20. H. S. Khesghi and L. E. Scriven, *Chem. Eng. Sci.* **46**, 519 (1991).
21. F. Brochard-Wyart, C. Redon and C. Sykes, *C. R. Acad. Sci. II* **314**, 19 (1992).
22. S. A. Safran and J. Klein, *J. Phys. II* **3**, 749 (1993).
23. G. Reiter, *Phys. Rev. Lett.* **68**, 75 (1992).
24. G. Reiter, *Langmuir* **9**, 1344 (1993).
25. A. Sharma and G. Reiter, *J. Colloid Interface Sci.* **178**, 383 (1996).
26. R. Yerushalmi-Rozen, J. Klein and L. J. Fetters, *Science* **263**, 793 (1994).